PCCP

Accepted Manuscript

ROYAL SOCIETY OF CHEMISTRY

www.rsc.org/pccp

Excluding Hyperconjugation from the Z Conformational Preference and Investigating its Origin: Formic Acid and Beyond

David Ferro-Costas[1]* and Ricardo A. Mosquera[1]

Abstract

Carboxylic acids, esters, secondary amides, and related molecules share a thermodynamic preference for the Z arrangement of their X=C—Y—R moiety. This conformational predisposition is known as the Z effect and its most common explanation invokes the hyperconjugation from a Y lone pair to the σ^*_{CX} orbital. In this work, we present clear topological evidences of that hyperconjugation is not responsible for the Z preference. Diverse tools defined within the Quantum Chemical Topology framework (as, for example, atomic and electron localization function populations or the interacting quantum atoms energy decomposition) were used to analyse the evolution of formic acid from the E conformer towards the Z conformation. Results highlight the important role of the π resonance in the barrier between conformers and they also indicate that the hyperconjugative interaction lacks of leading role. Concretely, in a X=C—Y—R structure, the X···R interaction seems to be the key to understand the preference for the Z arrangement of the moiety. Interestingly, our proposed explanation can be extended to a wide set of molecules presenting the same conformational preference, as proteins or peptide nucleic acids.

Keywords

z effect — formic acid — hyperconjugation — QTAIM

[1] *Departamento de Química Física, Universidade de Vigo, Facultade de Química, Lagoas-Marcosende s/n, 36310 Vigo, Galicia, Spain*

***Corresponding author**: davidferro@uvigo.es

1. Introduction

Experimental and computational studies established, long ago, that peptides exhibit a thermodynamical preference for the Z arrangement.[1] In this fashion, systems composed by units linked through peptide bonds are consequently affected by this Z predilection, being proteins or peptide nucleic acids (PNAs) important examples of biological significance. Interestingly, this conformational trend, named Z effect, is not only limited to peptide structures and, as a matter of fact, it can be found in esters, carboxylic acids, amides and related molecules (i.e. X=C—Y—R moieties, Figure 1).

As this effect is also presented in small systems, an interesting advantage rises: rigorous quantum mechanical methods can be used with them to delve into the basis (i.e. the electronic origin) of this conformational preference, leading to clearer ideas than those that could be achieved by analysing large systems, where such methods cannot be carried out yet, due to the consequent colossal computational cost, and/or where the huge amount of data could hide simple explanations.

Theoretical (and experimental) studies on RCOOR' molecules[2–4] (R,R' = H, CH_3) did not only confirm that the Z isomer is more stable than the E one, but they also considered this preference as an example of the famous anomeric effect.[5] Along those lines, diverse explanations were invoked to understand the Z preference that characterizes this effect as, for example: (i) steric repulsions,[6] (ii) lone pair repulsions,[7,8] (iii) dipole-dipole interactions,[9,10] or (iv) the acclaimed hyperconjugative interactions.[11] The last one, which proposes the overlap between the electron pair on the ether oxygen (lp_O) and the σ^* orbital of the C=O bond, notably rooted in the chemical community and it has been considered the preferred explanation for both the Z and the anomeric effects.[3] Thus, the Z effect is usually listed among those chemical facts where hyperconjugation can be invoked to obtain a successful explanation.

The achievements of the hyperconjugative model (HM) were so remarkable that, even nowadays, explanations based on it are still very popular among a wide part of the chemical community, even though hyperconjugation is not a physical observable but a consequence derived from the shortcomings affecting the frameworks of chemical bond. In fact, it is even not unusual to find the term "hyperconjugative interaction" in chemical literature, sprinkling some physical meaning on, possibly, the most precious mathematical objects within chemistry: the molecular orbitals.

Probably, the first conceptual problem associated to the hyperconjugative explanation appears when we come back to the biological systems. The N atom in a peptidic bond lacks a lone pair of electrons at the OCN plane, which invalidates the extension of the hyperconjugative origin to the Z preference in PNAs or proteins. Moreover, during the last decades, studies carried out with modern electron density analysis methods, which deal with a real observable (electron density), such as the prestigious quantum theory of atoms in molecules (QTAIM),[12–15] or with methods

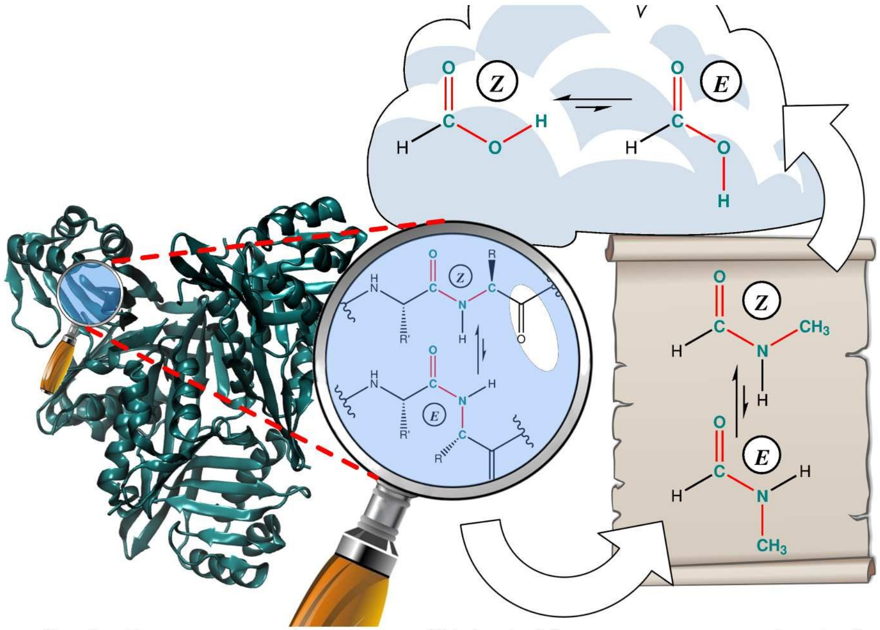

Figure 1. The preference for the Z arrangament in systems of biological importance, as proteins, is chemically equivalent to that of amides. Other related compounds, as carboxylic acids, also exhibit this same conformational trend.

based on the expansion of the wave function in terms of Lewis structures, as the famous valence bond theory,[16] have given rise to a growing number of evidences that directly question the reliability of the HM.[17–25] Thus, and referring only to conformational preferences, alternative intepretations have been presented for the anomeric effect,[18–21,24,25] the benzylic effect,[26] and even for the one at issue in this paper: the Z effect.[22]

We think it is of importance to revisit the origin of this effect making use of an extensive group of methods included in what is called Quantum Chemical Topology (QCT).[27] In this exhaustive research we deeply analyse this effect in the formic acid, our modelic system exhibiting Z preference. Although this system was used in previous works,[22] this is the first time we approach this effect using all our available QCT tools, which will certainly enrich previous electron density interpretations exclusively based on QTAIM descriptions.

2. Topological Tools

In this section, we will briefly introduce those tools included in the QTC that we have used. We will try to focus our explanation on concepts, skipping mathematical definitions unless it is strictly needed.

2.1 Atoms-in-molecules and bond properties

Bader's theory of atoms in molecules (QTAIM) has been used to define the limits of the atoms within a molecule. As in the density functional theory (DFT), the molecular electron density (ρ) is the cornerstone of this theory.[12,13] Concretely, the atoms are defined as regions of the three-dimensional space bounded by a zero-flux surface (zfs) in the gradient of ρ.

Interestingly, when two of these atoms are topologically bonded (i.e. they share a common interatomic zfs), an special kind of critical point in ρ, identified with an element of chemical structure, appears: the so-called bond critical point (bcp). Within Bader's theory, chemical bonding interactions are characterized and classified according to the properties of the electron and energy densities at the bcp, collectively known as "bond properties". For our purposes, we will analyse the electron density at the BCP (ρ_b), which is a reflection of the strength of a chemical bond.

2.2 Atomic and ELF populations

Let us consider the division of our molecule into a set of disjoint regions, $\{\Omega_i\}$. The electron population of Ω_i is given by the integral of the electron density over it:

$$N(\Omega_i) = N_{\Omega_i} = \int_{\Omega_i} d\mathbf{r}\rho(\mathbf{r}) \qquad (1)$$

and the set of Ω_i-populations recovers the total number of electrons in the system: $N = \sum_i N_{\Omega_i}$.

An example of a partition is the previous commented QTAIM,[12] which identifies each Ω_i with a basin of attraction of ρ, giving rise to atomic basins. The electron population of an atomic basin is known as its "atomic population".

Another interesting partition is the one induced by the topology of the electron localization function (ELF).[28,29] This function is a simple measure of electron localization in atomic and molecular systems and the partition of $\mathbb{R}^3$ into ELF basins of attraction reminds the Lewis structure of the molecule. Moreover, the electron population of these ELF basins is, generally, close to two electrons, reinforcing the idea of that ELF recovers the two-electron structure of the molecule.

2.3 Delocalization indices

In Lewis structures, the number of electrons associated to a given atom could be divided into localized and shared electrons. With a similar perspective, atomic populations can be divided into two contributions: one accounting for the localized electrons in the atom (λ_Ω) and another accounting for the number of delocalized electrons ($\delta_{\Omega\Omega'}$):[30–35]

$$N_\Omega = \lambda_\Omega + \sum_{\Omega' \neq \Omega} \delta_{\Omega\Omega'} \tag{2}$$

Concretely, given two atomic basins Ω and Ω', their delocalization index, $\delta_{\Omega\Omega'}$, is a quantitative measure of the number of shared electron pairs between them and it can be obtained through the exchange-correlation part of the second-order reduced density matrix (ρ_2^{xc}) according to:

$$\delta_{\Omega\Omega'} = -2 \int_\Omega d\mathbf{r}_1 \int_{\Omega'} d\mathbf{r}_2 \rho_2^{xc}(\mathbf{r}_1, \mathbf{r}_2) \tag{3}$$

These delocalization indices play, in orbital-free theories of the chemical bond, the same role as bond orders in conventional molecular orbital treatments.[36]

2.4 Statistic of the distribution of electrons

The square of the wave function of the system, $\Gamma = \Psi^*\Psi$, can be used to obtain the probability of a given event. Concretely, for a system of N electrons, $\Gamma(x_1,...,x_N)dx_1...dx_N$ gives us the probability of having electron 1 at dx_1, ..., and electron N at dx_N, where x is understood as a combined space-spin coordinate. Similarly, integrating over the corresponding basins, we can obtain the probability of finding simultaneously n_A electrons within atomic basin Ω_A , n_B electrons within Ω_B, ..., and n_M electrons within Ω_M, where n_A to n_M are integers which sum up to the total number of electrons, $\sum_{i=A}^{M} n_i = N$. Each partition of the N electrons leads to a real space resonance structure (RSRS), resembling a classical Pauling resonance structure, whose probability is given by:[37]

$$p(n_A, n_B, ...n_M) = \frac{N!}{\Pi_{i=A}^{M} n_i!} \int_D d\tau \Psi^* \Psi = \mathcal{N} \int_D d\tau \Gamma \tag{4}$$

where $\mathcal{N}$ is a combinatorial factor in charge of indistinguishability and D is a domain in which the first n_A electrons are integrated over Ω_A, the second n_B electrons over Ω_B, ..., and the last n_M electrons over Ω_M. The electron distribution function (EDF)[37–41] is defined by the collection of all the probabilities for each RSRS.

2.5 Interacting quantum atoms

Nature has provided us with electrons that can be described with two-particle interactions only. Thus, the averaged energy of a molecule can be obtained using, exclusively, its first reduced density matrix (1-rdm) and its pair density (ρ_2).[42]

The partition of the space into atomic basins also leads to the division of functions into atomic contributions. Splitting both the 1-rdm and ρ_2 using QTAIM basins allows the partition of all the energy components into intra- and interatomic contributions. Thus, the energy of a system can be written as:[43]

$$E = \sum_i E_{net}(\Omega_i) + \sum_{i>j} \sum_j V_{int}(\Omega_i, \Omega_j) \tag{5}$$

where the net energy of each atom, $E_{net}(\Omega_i)$, contains all the terms taking place exclusively in the atom, whereas the interaction energy between each pair of atoms, $V_{int}(\Omega_i, \Omega_j)$, is the collection of those terms including two different atomic basins. This interaction energy is normally written as a sum of two contributions, one containing all the interatomic interaction energies depending on $\rho(\mathbf{r})$, in what we call V_{clas}, and another accounting for the exchange-correlation part of the pair density, V_{xc}:

$$V_{int}(\Omega_i, \Omega_j) = V_{clas}(\Omega_i, \Omega_j) + V_{xc}(\Omega_i, \Omega_j) \tag{6}$$

As a consequence of this interacting quantum atoms (IQA) scheme,[43,44] a system can be analysed in terms of its constituent atoms and the interaction among them, which gives an intuitive idea of how a system works in terms of a classical conception of the Chemistry, devoid of orbital definitions.

3. System and Software

We will analyse the prototypical formic acid, as it is the simplest molecule exhibiting the Z effect. As the role of geometry relaxation is recommended to be decoupled from that of rigid rotation to analyse the effects of hyperconjugative interactions,[45,46] we will consider the optimized E structure and the rigid rotation from it towards the Z arrangement. The geometrical relaxation from the previous conformation towards the Z conformer will be analysed in a separated step.

Monodeterminantal Hartree-Fock (HF) wave functions were obtained with `Gaussian` (v09)[47] using the standard 6-311++ (2d,2p) 6d basis set. Bond properties and atomic populations were computed using the `AIMPAC` package,[48,49] whereas `Multiwfn`[50] was used for ELF populations. Finally, both the EDF and the IQA scheme were calculated using `EDF`[41,51] and `PROMOLDEN`[43] codes, developed by the Quantum Chemistry group of Oviedo University.

As we noted in previous works,[22–24] the Z preference is appropriately described at the HF level. This fact can be confirmed by Figure 2, which contains the energy profiles obtained with HF and CCSD calculations for the rigid rotation. Moreover, the evolution of the electron density at the bcps and of QTAIM populations present the same trends with both methodologies. All these facts point towards a general origin for this preference that should be captured even when crude approximations are introduced, as the use of HF descriptions. Furthermore, these are not the only reasons to use the HF methodology. On the one side, DFT or perturbational methods can be used neither to obtain the EDF, nor to perform the IQA energy scheme. On the other side, CASSCF calculations to describe the molecule along the rigid rotation would lead to longer running times for both EDF and IQA schemes, without really introducing significant differences in the results. Finally, `Multiwfn` calculates the ELF according to its usual formulation, only well defined for monodeterminatal wave functions.

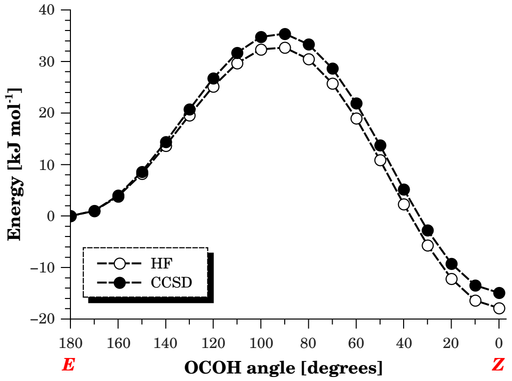

Figure 2. HF and CCSD energy profiles for the rigid rotation of the OCOH dihedral angle in formic acid.

4. Results

Along the whole rigid rotation from the E conformer, two other conformations are of interest: the one described by a OCOH dihedral angle around 90 degrees and the Z arrangement. According to traditional chemical knowledge, the OCO π resonance is broken in the first conformation, which would explain the energy barrier between the planar dispositions (Figure 2). On the other side, OCO hyperconjugation is more effective at 0 than at 180 degrees, which would justify the Z preference in formic acid.

It is necessary, then, to show the considered most significant Lewis structures (LSs) for our three important geometries. Both planar conformations are endowed with a resonance of the π electrons, normally indicated through the three LSs given in Figure 3a. Moreover, the Z structure presents an extra LS, IV, due to the σ resonance described by the $lp_O \rightarrow \sigma^*_{CO}$ hyperconjugative interaction, enhanced in this nuclear disposition (Figure 3b). Both effects are less effective in non-planar conformations and, hence, the perpendicular disposition would be mainly characterized only by LSs I and II (Figure 3a). Whenever possible, we will compare this description with the variation of diverse topological properties that our molecule overcomes upon rigid rotation from the E conformer.

(a) π resonance

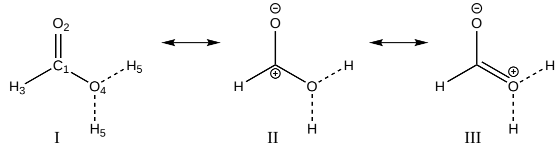

(b) σ hyperconjugation

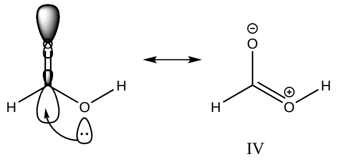

Figure 3. Resonance structures associated to the π resonance in both planar structures (a) and the extra structure associated to the σ resonance related to the hyperconjugative interaction in the Z structure (b).

4.1 Properties at bond critical points

Our molecule presents four bcps along the whole rigid rotation, one for each pair of atoms traditionally involved in a chemical bond. The evolution of the electron density at the bcps associated to the two C—O bonds (C1=O2 and C1—O4, see LS I in Figure 3a for atom labering) is shown in Figure 4. In it, we can see how ρ_b for the carbonyl bond finds its minimum value around 90 degrees, where the ether bond exhibits its maximum value. These two findings do not agree with the breaking of the π resonance in the OCO unit at this point, where the resonance hydrid at this point is understood as a combination of structures I and II, lacking the form III (Figure 3a). However, these topological results are based on magnitudes at bcps situated in the OCO plane and, hence, π-resonance effects are probably not visible at them.

Interestingly, we observe facts that are consistent with the idea of more effective hyperconjugative $lp_O \rightarrow \sigma^*_{CO}$ interaction in the Z arrangement, which should weaken the C1=O2 bond and reinforce the C1—O4 one. Thus, ρ_b for the carbonyl bond is smaller in the Z rigid conformation than in the E one, finding the opposite trend for the ether bond (Figure 4). Nevertheless, we are dealing with a local magnitude (calculated at a single point) and it could be more representative to obtain quantities arising from the consideration of different points, in order to better account for hyperconjugative interations and π resonances.

4.2 Evolution of atomic and ELF populations

The analysis of integrated magnitudes seems to be necessary after observing the results of the previous section. The first quantity of interest is the atomic population of each individual atom defining the OCO moiety, whose evolution

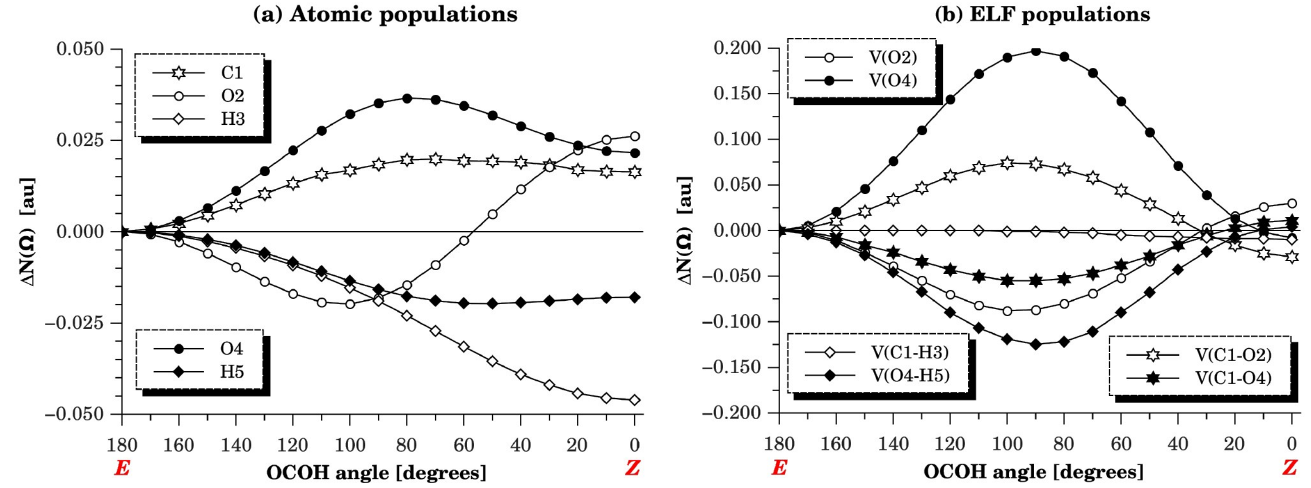

Figure 5. Evolution of atomic (a) and ELF basin (b) populations along rigid rotation from the E conformer.

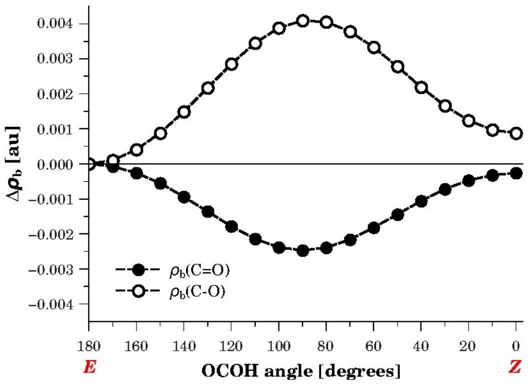

Figure 4. Evolution of the electron density at the bond critical point associated to both C-O bonds in the system: the carbonyl (black) and the ether (white) bonds.

is depicted in Figure 5a. Data at the perpendicular structure seem to correspond with the impossibility of the OCO π resonance: the atomic population of the carbonyl oxygen is smaller than at the E conformer and, oppositely, N_{O4} is larger. However, both oxygen atoms own more electron population at the Z disposition. Although the increase in the population of O4 could be thought as a consequence of a transference from its acid hydrogen, the whole OH moiety increases its electron population, meaning that the HCO fragment is displacing its electron density towards the OH, contrary to predictions based on the HM. In this manner, results suggest that, if this interaction really takes place, it does not really play an important role in the Z preference.

Nevertheless, the HM is very specific indicating which chemical elements are involved in the interaction. It could happen that hyperconjugative displacements of electron density were hidden in the total atomic population. This leads rapidly to think about the evolution of the electron population associated to ELF basins. Results are more pleasant in this case: ether oxygen lone pairs, $V(O4)$, exhibit smaller population at Z and, likewise, populations of ELF basins associated to C1=O2 and C1—O4 bonds behave according to the HM: the carbonyl bond owns less electrons in Z than in E, oppositely to the ether one.

Despite previous findinds, it should be said that the magnitudes associated to the HM are really slight. Let us consider a triad of numbers associated to the population variation of V(O4), V(C1-O2), and V(C1-O4) ELF basins. At 90 degrees this triad is (0.197,0.073,-0.055), which would describe the effects of the π-resonance breaking from the E conformer. However, we have (-0.008,-0.029,0.011) for the Z conformation. The three values are much smaller than those related to the π resonance and, however, the difference between the rigid Z structure and the E conformer accounts for -17.9 kJ·mol^{-1}, slightly larger than half of the rigid barried from E to Z (32.7 kJ·mol^{-1}).

4.3 Internal OCO delocalization index

The evolution of basin populations does not fit, in general, with the HM expectations. Nevertheless, it is tempting to think that maybe the effect of the hyperconjugation are exclusively associated to the delocalization in the OCO moiety and has a little impact on atomic and ELF populations. For this reason, we have also investigated the evolution of what could be called the intrinsic delocalization in the OCO, δ_{OCO}, which measures the delocalization among the atoms defining the OCO fragment. This amount can be obtained by the sum:

$$\delta_{OCO} = \delta_{C1,O2} + \delta_{C1,O4} + \delta_{O2,O4} \tag{7}$$

Once again, we observe (Figure 6a) agreement with the breaking of the π resonance in the first part of the rotation but the final value of δ_{OCO}, slightly smaller than that of the E conformer (2.171 vs 2.173 au), is not in line with hyperconjugative expectations.

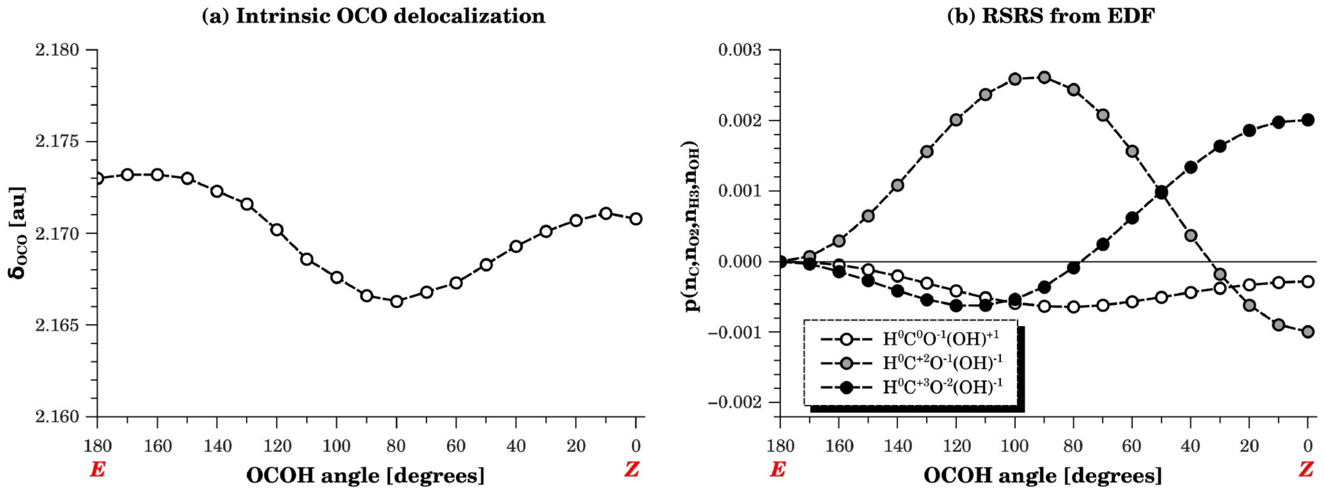

Figure 6. Evolution of the intrinsic delocalization in the OCO moiety (a) and of the probability of three RSRSs (b) along rigid rotation from the E conformer.

4.4 Resonance structure probabilities

As a final test related to how electrons are distributed in the space, we can obtain the evolution of certain RSRSs along rigid rotation. We will consider the division of our molecule into four regions: C1, O2, H3, and the OH fragment. The RSRS associated to Lewis resonance structures III and IV (Figure 3) is given by the vector $(n_C, n_{O2}, n_{H3}, n_{OH}) = (6, 9, 1, 8)$. Its evolution can be found in Figure 6b, together with those of the two most probable RSRSs, $H^0C^{+3}O^{-2}(OH)^{-1}$ and $H^0C^{+2}O^{-1}(OH)^{-1}$, given by $(3, 10, 1, 10)$ and $(4, 9, 1, 10)$, respectively. Firstly, we observe that the variation of the RSRS associated to both π and σ resonances is smaller than that of the most probable structures. Secondly, the probability of the hyperconjugative RSRS decreases at the perpendicular arrangement, in agreement with the reduced π resonance. Not surprisingly, this RSRS is more important in the E conformer than in the Z conformation, providing another topological evidence of the ineffectiveness of the hyperconjugative interaction.

4.5 The energetic origin of the Z preference

At this point, we have found that there are topological evidences supporting the breaking of the OCO π resonance in the halfway to the Z arrangement from the E conformer. However, the only signs that can be associated to the better hyperconjugative resonance in Z are of doubtful importance. We want to conclude this topological analysis of the rigid rotation of formic acid with the IQA energetic scheme. As we will see, it will present another indication of the small importance of hyperconjugation in the Z effect and it will offer the energetic origin of this conformational preference.

In order to continue the comparison to resonance effects, we should consider the division of our molecular system into two regions: the OCO moiety and the two hydrogen atoms. This leads to the next partition of the molecular energy:

$$E = E_{net}(OCO) + E_{net}(HH) + V_{int}(OCO, HH) \tag{8}$$

With this scheme, resonance effects associated to the OCO moiety should be visible through the $E_{net}(OCO)$ term.

The same pattern as in previous sections is found here: there are evidences for the π resonance, but not for the σ one. The evolution of $E_{net}(OCO)$ fits that of the total energy until the perpendicular structure is reached (Figure 7a). This clearly indicates that the energetic origin of the barrier takes place inside the OCO moiety, as it is predicted according to the π resonance. Conversely, $E_{net}(OCO)$ is almost identical at both planar arrangements, being slightly larger in the Z conformation (around 0.6 kJ·mol^{-1}). This is, the energy terms taking place inside the OCO moiety, where the hyperconjugation interaction should be included, point toward the incorrect preference for the E disposition.

The origin of the shape exhibited by $E_{net}(OCO)$ can be investigated by splitting this energy into three contributions: the non-interacting net energy of the OCO fragment, defined by the sum of the net energies of the components, $E^0_{net}(OCO) = E_{net}(C1) + E_{net}(O2) + E_{net}(O4)$, the classic interactions among the different atoms in OCO, $V_{clas}(OCO)$, and the exchange interaction, $V_x(OCO)$.[*] Meaningfully, the second one is the term that actually defines the shape of $E_{net}(OCO)$, as it can be seen in Figure 7b. Hence, the charge displacements associated to the π resonance breaking desestabilize the molecule through classical interactions, instead of altering significantly the exchange contribution, normally attributed to the bond formation.

Figure 7a also points out that the stabilizing origin of the Z structure lies on the interaction between the OCO and

---

[*] At HF level, there is no correlation energy. Hence, exchange-correlation terms (xc subscript) only present the exchange contribution (x subscript).

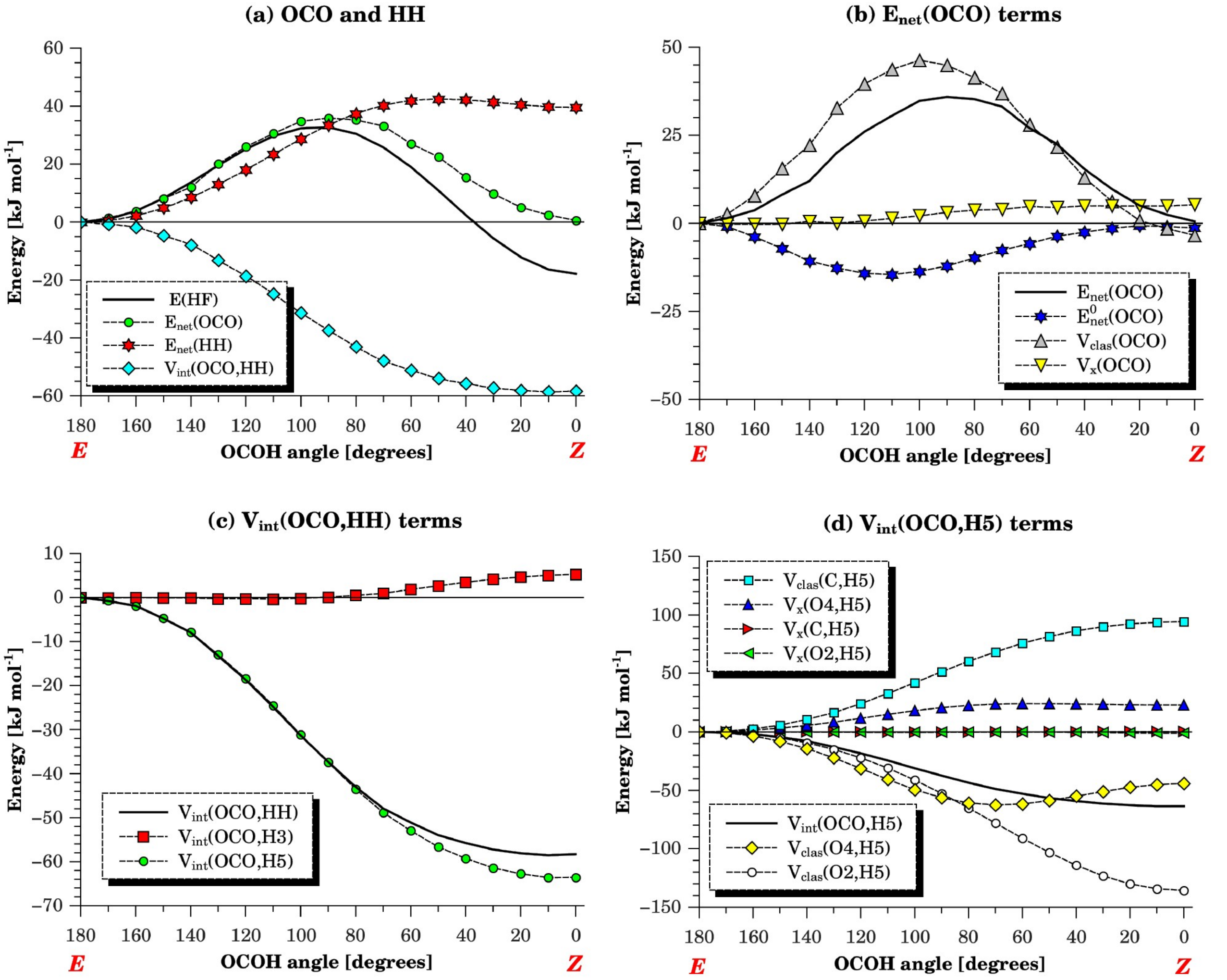

Figure 7. Evolution of diverse terms defined within the IQA scheme for the partitioning of the molecular energy along the OCOH rigid rotation from the E conformer.

the hydrogens. Actually, it is the interaction between the OCO and the acid hydrogen (H5) the one stabilizing the Z formic acid (Figure 7c). Its decomposition in different energy terms, Figure 7d, reflects the importance of the classical interaction between the carbonyl oxygen and the acid hydrogen (concretely, the attraction of the carbonyl oxygen electron density by the hydrogen nucleus). We highlight that also the interaction between the atoms in the OH bond are of importance (Figure 7d), but the O2···H5 interaction is clearly the key in this conformational trend. It is noteworthy that Mo proposed[17] also an electrostatic origin for a similar conformational preference (the anomeric effect), heretofore justified by an equivalent hyperconjugative interaction.

Interestingly, the importance of this interaction allows explaining why the Z preference is enhanced when changing the carbonyl oxygen (X=O) by a sulphur (X=S) or by a selenium (S=Se) atom, as indicated in a previous study.[22] The electron density of these atoms is larger than that of oxygen, which permits enhancing the X2···H5 interaction. In this manner, the energy differences between the rigid Z arrangement and the E conformer are -21.1 kJ·mol^{-1} for S and -22.4 kJ·mol^{-1} for Se, whereas it was -17.9 kJ·mol^{-1} for O. We remark that the qualitative use of the HM leads us to the opposite trend, as the delocalization of the oxygen lone pair in the σ^*_{CX} orbital should be less effective.[22]

4.6 Towards geometry relaxation

Finally, it can be of interest to examine how all the previous quantities vary from the final frozen conformation to the relaxed one. Results are contained within Table 1, where we observe that:

- the C=O bond enlarges whereas the C—O one shrinks;
- in line with the previous observation, ρ_b associated to the C=O bond decreases, whereas it increases for the ether bond;

- upon relaxation, both the ether and the carbonyl oxygens endow less electron population;
- the electron populations associated to lone pairs of the ether oxygen and to the C=O bond decrease, whereas the one of the C—O bond increases;
- although the previous point is in line with the HM, the amount associated to the O4 lone pairs is really small and it is also lower than the increase in the C—O bond;
- the intrinsic delocalization index in the OCO moiety increases just 0.001 au upon relaxation;
- there is no appreciable variation in the probability of the RSRS associated to Lewis structures III and IV (Figure 3);
- both the OCO and the HH moieties are stabilized upon relaxation, whereas its interaction is less favourable

Although some of the previous observations are not in line with the hyperconjugative interaction, a few of them seem to support it. Consequently, the hyperconjugative interaction is not necessarily excluded in the geometrical relaxation. Thus, whereas the origin of the preference for the Z arrangement does not lie in the $lp_O \rightarrow \sigma^*_{CO}$ hyperconjugative interaction, the geometrical variation could still be ascribed to it.

It is of importance to notice that these geometrical relaxation decreases the energy of the Z conformation by just 2.6 kJ·mol^{-1}, whereas the rigid rotation accounts for -17.9 kJ·mol^{-1}.

Table 1. Variation in different properties (P) upon geometrical relaxation from the Z rigid conformation. Bond distances (d_{i-j}) are in Å, whereas energies are in kJ·mol^{-1}. The rest of the magnitudes are in au.

$\Delta P = P_{Zrelax} - P_{Zrigid}$			
$\Delta d_{C=O}$:	0.006	ΔE_{HF} :	-2.6
Δd_{C-O} :	-0.006	$\Delta E_{net}(OCO)$:	-6.8
Δd_{C-H} :	-0.006	$\Delta E_{net}(HH)$:	-9.9
Δd_{O-H} :	0.005	$\Delta V_{int}(OCO,HH)$:	14.1
$\Delta \rho_b(C=O)$:	-0.0064	$\Delta \delta_{OCO}$:	0.001
$\Delta \rho_b(C-O)$:	0.0049	$\Delta p(6,9,1,8)$:	0.000
ΔN_{C1} :	-0.007	$\Delta N_{V(O2)}$:	0.029
ΔN_{O2} :	-0.004	$\Delta N_{V(O4)}$:	-0.002
ΔN_{H3} :	0.011	$\Delta N_{V(C1-O2)}$:	-0.025
ΔN_{O4} :	-0.005	$\Delta N_{V(C1-H3)}$:	-0.003
ΔN_{H5} :	0.005	$\Delta N_{V(C1-O4)}$:	0.009
		$\Delta N_{V(O4-H5)}$:	-0.008

5. Conclusions

We present here strong evidences of that the hyperconjugative interaction between the lone pair of the ether oxygen and the $\sigma^*_{C=O}$ molecular orbital is not responsible of the Z preference in formic acid. Data based on topological tools point towards the interaction between the carbonyl oxygen and the acid hydrogen as the leading interaction favoring this conformation. Moreover, this explanation can be extended *mutatis mutandis* to explain this conformational preference in amides or in even more exotic species, as PNAs or proteins, where the hyperconjugative interaction could not be invoked.

Acknowledgments

D. F-C. also thanks Spanish Ministry of Education for an FPU fellowship.

References

[1] S. S. Zimmerman and H. A. Scheraga, *Macromolecules*, 1976, **9**, 408–416.

[2] A. J. Kirby, *The Anomeric Effect and Related Stereoelectronic Effects at Oxygen*, Springer-Verlag, Berlin, 1983.

[3] E. Juaristi and G. Cuevas, *The Anomeric Effect*, CRC Press: Boca Ratón, Florida, 1995.

[4] E. L. Eliel, N. L. Allinger, S. J. Angyal and G. A. Morrison, *Conformational Analysis*, American Chemical Society, Washington, 1981.

[5] J. T. Edward, *Chem. Ind. (London)*, 1955, **36**, 1102–1104.

[6] E. S. Gould, *Mechanism and Structure in Organic Chemistry*, Holt, Rinchart and Winston, New York, 1959.

[7] D. Cook, *J. Am. Chem. Soc.*, 1958, **80**, 49–55.

[8] N. L. Owen and N. Sheppard, *Proc. Chem. Soc.*, 1963, 264–265.

[9] J. E. Piercy and S. V. Subrahmanyam, *J. Chem. Phys.*, 1965, **42**, 1475–1479.

[10] H. Wennerstrom, S. Forsen and B. Roos, *J. Phys. Chem.*, 1972, **76**, 2430–2436.

[11] J. R. Larson, N. D. Epiotis and F. Bernardi, *J. Chem. Phys.*, 1978, **100**, 5713–5716.

[12] R. F. W. Bader, *Atoms in Molecules: A Quantum Theory*, Clarendon Press, Oxford, 1995.

[13] C. F. Matta and R. J. Boyd, *The Quantum Theory of Atoms in Molecules: From Solids State to DNA and Drug Design*, Wiley-VCH, 2007.

[14] R. F. W. Bader, *Chem. Rev.*, 1991, **91**, 893–928.

[15] R. F. W. Bader, *J. Phys. Chem. A*, 2010, **114**, 7431–7444.

[16] D. Cooper, *Valence bond theory*, Elsevier Science, Amsterdam, The Netherlands, 2002.

[17] Y. Mo, *Nat. Chem.*, 2010, **2**, 666–671.

[18] A. Vila and R. A. Mosquera, *J. Comput. Chem.*, 2007, **28**, 1516–1530.

[19] K. Eskandari, A. Vila and R. A. Mosquera, *J. Phys. Chem. A*, 2007, **111**, 8491–8499.

[20] A. Vila and R. A. Mosquera, *Chem. Phys. Lett.*, 2007, **443**, 22–28.

[21] A. Vila, L. Estévez and R. A. Mosquera, *J. Phys. Chem. A*, 2011, **115**, 1964–1970.

[22] D. Ferro-Costas, N. Otero, A. M. Graña and R. A. Mosquera, *J. Comput. Chem.*, 2012, **33**, 2533–2543.

[23] D. Ferro-Costas and R. A. Mosquera, *J. Phys. Chem. A*, 2013, **117**, 257–265.

[24] D. Ferro-Costas, A. Vila and R. A. Mosquera, *J. Phys. Chem. A*, 2013, **117**, 1641–1650.

[25] D. Ferro-Costas and R. A. Mosquera, *J. Chem. Theory Comput.*, 2013, **9**, 4816–4824.

[26] A. Vila, M. G. Bugarín and R. A. Mosquera, *J. Phys. Chem. A*, 2011, **115**, 13088–13095.

[27] P. L. Ayers, R. J. Boyd, P. Bultinck, M. Caffarel, R. Carbó-Dorca, M. Causá, J. Cioslowski, J. Contreras-Garcia, D. L. Cooper, P. Coppens, C. Gatti, S. Grabowsky, P. Lazzeretti, P. Macchi, Á. M. Pendás, P. L. A. Popelier, K. Ruedenberg, H. Rzepa, A. Savin, A. Sax, W. H. E. Schwarz, S. Shahbazian, B. Silvi, M. Solà and V. Tsirelson, *Comput. Theor. Chem.*, 2015, **1053**, 2 – 16.

[28] A. D. Becke and K. E. Edgecombe, *J. Chem. Phys.*, 1990, **92**, 5397 – 5403.

[29] A. Savin, R. Nesper, S. Wengert and T. F. Fässler, *Angew. Chem. Int. Ed. Engl.*, 1997, **36**, 1808 – 1832.

[30] R. Daudel, R. F. W. Bader, M. Stephens and D. S. Borrett, *Can. J. Chem.*, 1974, **52**, 1310–1320.

[31] R. F. W. Bader and M. E. Stephens, *J. Am. Chem. Soc.*, 1975, **97**, 7391–7399.

[32] R. Ponec and M. Strnad, *Int. J. Quantum Chem.*, 1994, **50**, 43–53.

[33] R. Ponec and F. Uhlik, *J. Mol. Struct. (THEOCHEM)*, 1997, **391**, 159–168.

[34] X. Fradera, M. A. Austen and R. F. W. Bader, *J. Phys. Chem A*, 1999, **103**, 304–314.

[35] D. Ferro-Costas and R. A. Mosquera, *Phys. Chem. Chem. Phys.*, 2015, **17**, 7424–7434.

[36] A. Martín Pendás, M. A. Blanco and E. Francisco, *J. Chem. Phys.*, 2006, **125**, 184112.

[37] E. Chamorro, P. Fuentealba and A. Savin, *J. Comput. Chem.*, 2003, **24**, 496 – 504.

[38] E. Cancès, R. Keriven, F. Lodier and A. Savin, *Theor. Chem. Acc.*, 2004, **111**, 373 – 380.

[39] E. Francisco, A. Martín Pendás and M. A. Blanco, *J. Chem. Phys.*, 2007, **126**, 094102.

[40] A. Martín Pendás, E. Francisco and M. A. Blanco, *J. Chem. Phys.*, 2007, **127**, 144103.

[41] E. Francisco and A. Martín Pendás, *Comput. Phys. Commun.*, 2014, **185**, 2663 – 2682.

[42] R. McWeeny, *Methods of Molecular Quantum Mechanics*, Academic Press, London, 1992.

[43] M. A. Blanco, A. M. Pendás and E. Francisco, *J. Chem. Theory Comput.*, 2005, **1**, 1096–1109.

[44] E. Francisco, A. Martín Pendás and M. A. Blanco, *J. Chem. Theory Comput.*, 2006, **2**, 90–102.

[45] F. M. Bickelhaupt and E. J. Baerends, *Angew. Chem. Int. Ed.*, 2003, **42**, 4183–4188.

[46] A. Martín Pendás, M. A. Blanco and E. Francisco, *J. Comput. Chem.*, 2009, **30**, 98–109.

[47] M. J. Frisch, G. W. Trucks, H. B. Schlegel, G. E. Scuseria, M. A. Robb, J. R. Cheeseman, G. Scalmani, V. Barone, B. Mennucci, G. A. Petersson, H. Nakatsuji, M. Caricato, X. Li, H. P. Hratchian, A. F. Izmaylov, J. Bloino, G. Zheng, J. L. Sonnenberg, M. Hada, M. Ehara, K. Toyota, R. Fukuda, J. Hasegawa, M. Ishida, T. Nakajima, Y. Honda, O. Kitao, H. Nakai, T. Vreven, J. A. Montgomery, Jr., J. E. Peralta, F. Ogliaro, M. Bearpark, J. J. Heyd, E. Brothers, K. N. Kudin, V. N. Staroverov, R. Kobayashi, J. Normand, K. Raghavachari, A. Rendell, J. C. Burant, S. S. Iyengar, J. Tomasi, M. Cossi, N. Rega, J. M. Millam, M. Klene, J. E. Knox, J. B. Cross, V. Bakken, C. Adamo, J. Jaramillo, R. Gomperts, R. E. Stratmann, O. Yazyev, A. J. Austin, R. Cammi, C. Pomelli, J. W. Ochterski, R. L. Martin, K. Morokuma, V. G. Zakrzewski, G. A. Voth, P. Salvador, J. J. Dannenberg, S. Dapprich, A. D. Daniels, Ö. Farkas, J. B. Foresman, J. V. Ortiz, J. Cioslowski and D. J. Fox, *Gaussian 09 Revision A.02*, Gaussian Inc. Wallingford CT 2009.

[48] R. F. W. Bader, *AIMPAC: A Suite of Programs for the AIM Theory*, McMaster University: Hamilton, Ontario, Canada.

[49] F. W. Biegler-König, R. F. W. Bader and T.-H. Tang, *J. Comput. Chem.*, 1982, **3**, 317 – 328.

[50] T. Lu and F. Chen, *J. Comput. Chem.*, 2012, **33**, 580 – 592.

[51] E. Francisco, A. Martín Pendás and M. A. Blanco, *Comput. Phys. Commun.*, 2008, **178**, 621 – 634.